A sidelong look at storm tracks

I. N. James* and Ulrike Burkhardt[†]
School of Mathematics, Meteorology and Physics, University of Reading, Reading RG6 6AF, UK

*Correspondence to:
I. N. James, School of
Mathematics, Meteorology and
Physics, University of Reading,
Reading RG6 6AF, UK.
E-mail: I.N.James@reading.ac.uk*

Abstract

The three-dimensional structure of time-mean eddy statistics and the time evolution of longitude-height sections suggest that the storm tracks form a single structure in the upper troposphere and indicate that eddies regularly propagate from the Pacific to the Atlantic. The model of storm tracks as independent meta-systems is inadequate. Copyright © 2006 Royal Meteorological Society

1. Introduction

The distribution of high frequency transient eddy activity in the troposphere takes the form of elongated maxima, and these maxima roughly coincide with the tracks taken by low-level depression systems (Blackmon, 1976; Wallace *et al*., 1988; Hoskins and Hodges, 2002). Consequently, these maxima have been called 'storm tracks'. Here, 'high frequency' means periods of less than 6–8 days. In the Northern hemisphere, two storm tracks are recognised, one starting over the Pacific coast of East Asia and extending across the Pacific, and the other starting over the east coast of North America and extending across the Atlantic. The Southern Hemisphere has a single, longer storm track, beginning in the mid-Atlantic and extending to the south of Australia (see, e.g. Trenberth, 1991; James and Anderson, 1984). Chang *et al*. (2002) give a comprehensive review of the observations, theory and modelling of storm tracks.

A conceptual model of the storm track structure was provided by the lifecycle calculations of Simmons and Hoskins (1978, 1980). Starting from a normal mode initial disturbance, they showed that for a variety of realistic zonal jets, baroclinic waves underwent a sequence of growth, maturity and decay. Growth is characterised by large poleward and upward temperature fluxes, particularly in the lower troposphere, associated with the baroclinic instability process. Decay is characterised by large poleward momentum fluxes in the upper troposphere. Such fluxes are associated with the radiation of Rossby waves to low latitudes from the baroclinically active zones.

A similar variation of eddy transport properties is observed as one moves eastwards along the storm track regions. The western part of the storm track is dominated by large low-level temperature fluxes. This region is where, on average, systems are intensifying. These fluxes are smaller towards the eastern part of the storm track where instead the upper tropospheric momentum fluxes become large. Here cyclonic weather systems tend to decay and there is a propensity for anticyclonic blocks to form.

With a life cycle conceptual model as background, authors such as Hoskins and Valdes (1990) have linked the storm track location to local properties of the time-mean flow, such as the location of jets, variations of vertical shear and static stability and the mean distribution of diabatic processes. In particular, Hoskins and Valdes (1990) showed a good correlation between the growth rate of the most unstable disturbances according to the Eady linear instability theory, $(f/N)\partial U/\partial z$, and the observed distribution of eddy temperature fluxes. Using these ideas, the concept has grown up of the storm tracks as relatively isolated large scale 'meta-systems', comprising a number of synoptic scale transient weather systems, each undergoing a non-linear baroclinic lifecycle, and possibly pre-conditioning the flow for further baroclinic events.

Many of these studies have been hampered by the range of diagnostic graphical tools readily available for analysis. For example, many of the studies (e.g. Hoskins *et al*., 1983) have inferred the three-dimensional structure of the storm track from data at two pressure levels, one characteristic of the lower troposphere and one characteristic of the upper troposphere or tropopause region. One aim of this article is to delineate the three-dimensional structure of the storm tracks, while making only minimal assumptions about the structures present. When this is done, a second question immediately arises. The storm tracks are not sharply differentiated from the rest of the mid-latitude tropospheric circulation. How then do the storm tracks interact with their surroundings? An important element of this interaction is the nature of

[†] DLR Institut für Physik der Atmosphäre, Oberpfaffenhofen, Germany.
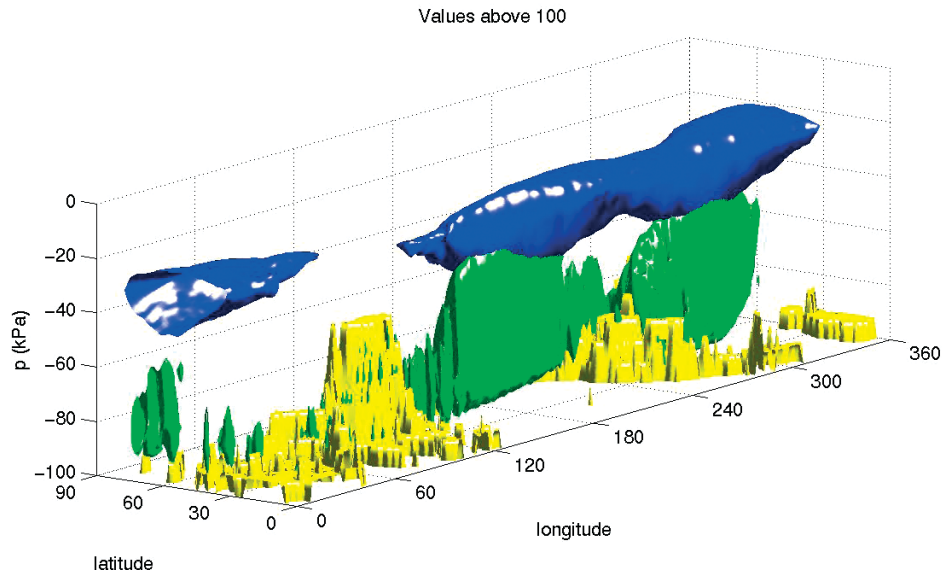
Figure 1. The Northern Hemisphere storm track in the DJF season. The blue surface encloses values of high pass filtered eddy kinetic energy in excess of 100 m^2 s^{-2}, and the green surface values of downward temperature flux less than -0.2 kPa s^{-1}. The yellow surface encloses regions beneath the land surface

disturbances at the start of the storm track that trigger the subsequent baroclinic developments. Where do they originate and how do they form? These questions lead us to the main theme of this article; namely, that there are strong linkages between the Pacific and Atlantic storm tracks, and it may be misleading to treat them as separate, independent, hyper-weather systems.

2. Data

The study in this article is based on ECMWF re-analysis (ERA) data (Uppala *et al.*, 2005). The re-analysis project has used a consistent analysis forecast system to re-process data collected by ECMWF since its inception in 1979. The fields are initialised to suppress spurious gravity wave activity and to provide an estimate of vertical motion. The data have been extracted on a 1.75 grid, and on 17 pressure surfaces every 12 h.

For the purpose of storm track studies, the data have been used to construct filtered time series of transient eddy quantities for the December–January–February season, i.e. for the Northern Hemisphere winter. The filtering employed a 31 point Lanzcos filter, and the filter window for the data used in this article was 2 to 6 days. Various lower frequency band and low pass filters were also used.

3. Distribution of transient eddy activity

The traditional view of the storm tracks is summarised in James (1995), Chapter 5. Here, plots of various seasonal mean eddy variance and co-variance quantities, filtered with a 2–6 day band-pass filter and plotted on isobaric surfaces, generally show two centres of eddy

activity, one over the Pacific and one over the Atlantic ocean.

Figure 1 shows an attempt to present a three-dimensional representation of the storm track. Perspective views of two iso-surfaces are shown. One is an iso-surface of high frequency transient eddy kinetic energy, denoted by blue. This shows maximum values in the upper troposphere, with largest values over the oceans and smaller values over the central parts of the Eurasian landmass. At lower levels, the volume branches into two maxima, one over each ocean basin, but near the tropopause; it essentially encloses a single maximum. The eddy kinetic energy close to its maximum near the tropopause varies by not more than 15% between the ocean basins and the centre of North America, compared with variation of a factor of more than two at lower levels. This diagram is consistent with the feature tracking results of Hoskins and Hodges (2002), which reveal a single spiral concentration of upper level vortices winding around the entire Northern Hemisphere, but with a weakening over Central Asia.

The green iso-surfaces enclose strong values of upward transient temperature flux. These fluxes are very small over the continents, but large over the ocean basins. The upward temperature fluxes are closely related to the integrand of the integral for generation of eddy kinetic energy:

$$CE = \int_V \left(-\frac{R}{p}\overline{[\omega^* T^*]} \right) dV \qquad (1)$$

Figure 1 suggests that the source of eddy kinetic energy is located over the mid-latitude Pacific and Atlantic Oceans, and that these two sources feed a single reservoir of eddy kinetic energy in the upper troposphere. The distinction between the Pacific and

Hovmoeller plot–v' at 25 kPa, 1984–5
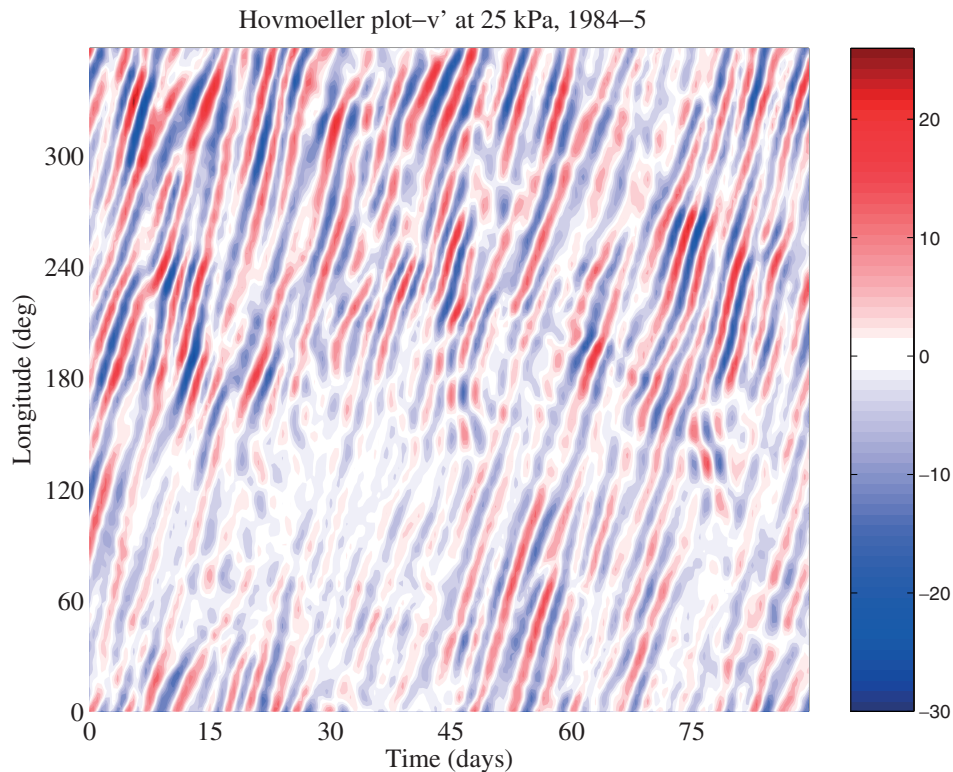
Figure 2. Hovmöller plot of band-pass filtered meridional wind *v'* at 25 kPa for DJF, 1984–1985

Atlantic storm tracks becomes systematically less marked as one considers higher levels in the troposphere. Rather than the suggestion of two independent storm tracks, the notable feature of this plot is the interruption of the single storm track at low levels over North America.

4. The contribution of individual disturbances

Figure 1 gives a static, Eulerian time average representation of the Northern Hemisphere storm tracks. We turn now to examine the way in which these structures are built up by the accumulation of individual eddy events. Figure 2 shows a longitude-time plot (a so-called 'Hovmöller plot') for a single season, December 1984 to February 1985, from the ERA time series. The plot shows the fluctuating part of the 25 kPa poleward component of wind, *v'*, averaged from 40°N to 60°N, and band-pass filtered to include only disturbances of periods 2 to 6 days. The latitude averaging was introduced to capture the eastward progression of disturbances even when there was a poleward component to their propagation. The generally west to east progression of disturbances is clearly seen. The data were extracted every 0.5 days, an interval which generally suffices to record the movement of systems adequately. However, in a few places (e.g. near longitude 135°, days 75 to 85), there appears to be retrogression of disturbances: this is an artefact caused by aliasing of rather fast moving disturbances on the coarse time grid.

A number of points arise from this diagram. First, the two storm tracks are easily discerned, as regions where the fluctuations in *v'* are unusually strong. As might be expected from Figure 1, the distinction between the two storm tracks is not always pronounced. The Pacific storm track extends from 130E to around 200E. However, it is strongest in the transition seasons, at the start and end of the time series, and relatively weak in midwinter. The Atlantic storm track extends from 270E to the Greenwich meridian. Here, the strongest disturbances are in midwinter. The contrasting seasonal cycle of the two storm tracks is well known; see, e.g. Nakamura (1992).

Secondly, it is worth noting that the storm track consists of a rather small number of individual events. In this example, the Atlantic storm track is made up of some 17 individual trough-ridge systems near the Greenwich meridian. Eulerian statistics, such as those used to compile Figure 1, are relatively stable for averaging periods of more than a month or so, despite the small number of major events that contributes to the time average.

However, the most remarkable feature of this diagram, one that has not, so far as we are aware, been remarked upon by other authors, is the longevity of the individual disturbances. Individual trough or ridge systems can be followed far out of the storm track regions. In fact, almost no examples of disturbances amplifying *in situ* in the storm tracks from small amplitude to large can be identified. In virtually every case of a strong storm track disturbance, precursor disturbances

(a)

(b)

(c)
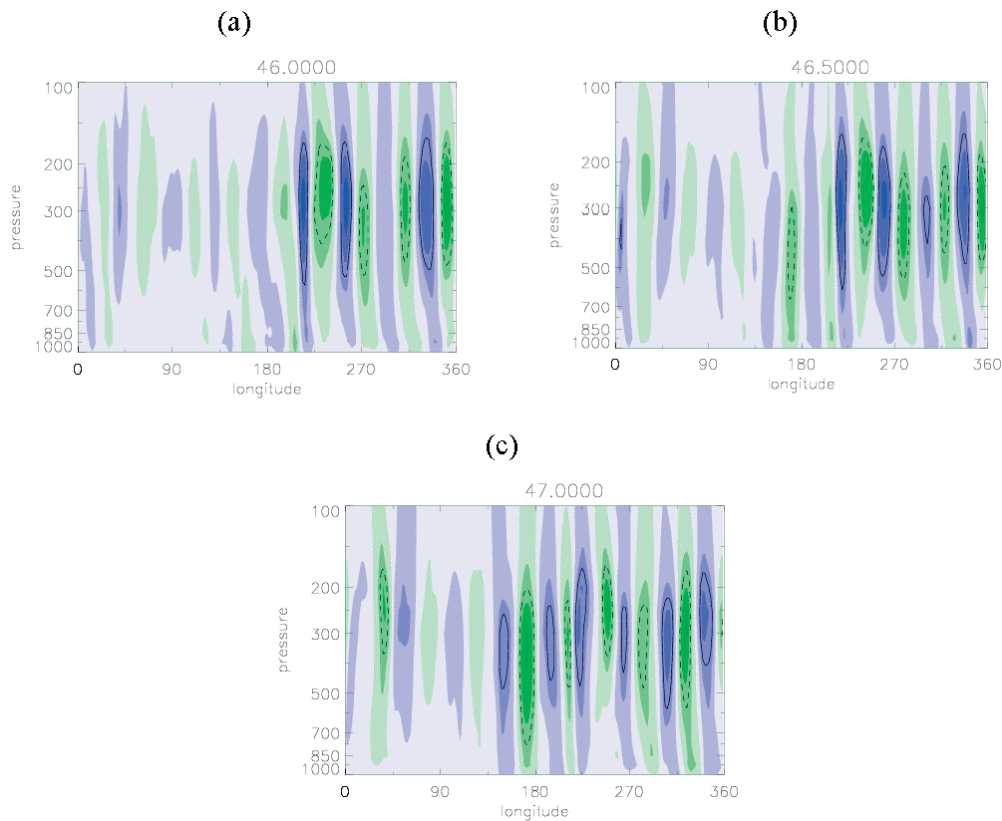
Figure 3. A sequence of longitude-height sections of the high pass filtered meridional wind for the DJF 1984–1985 season, ERA data. Colour scale as Figure 2. (a) day 46.0, (b) day 46.5 and (c) day 47. Note the intensification of disturbances and the increase of the westward phase tilt with height below 70 kPa as the main disturbances pass 270 °E

can be seen far upstream of the storm track, propagating eastward and amplifying to varying degrees within the storm track. Particularly noteworthy are the transition season events, around days 0 to 10 and again from days 60 to 70, when disturbances passing out of the Atlantic storm track can be followed right across Asia, into the Pacific storm track, and thence back into the Atlantic. Individual trough or ridge systems apparently persist for 20 or 30 days, far beyond the usual limits of synoptic predictability.

Figure 3 shows a sequence of longitude-height sections of v' at the time of one particular flare up of eddy activity in the Atlantic storm track. The general eastward progression of eddies is clear, as is their intensification in the 270–360 °E sector. As the disturbances enter the storm track region, a westward phase tilt develops with height and intensifies in the lower troposphere. Such a phase tilt with height of the v' fields indicates systematic poleward temperature fluxes (see e.g. James 1995, pp122 *et seq*). In their turn, the temperature fluxes, in conjunction with a poleward temperature gradient, indicate a baroclinic source of eddy kinetic energy. We term this increasing phase tilt and intensification of the disturbances 're-ignition'. Characteristic of virtually every development of eddies in the time series of v' that we have studied is such a re-ignition of baroclinic energy conversions, signalled by increasing phase tilt, as roughly barotropic disturbances move into the storm track regions.

Finally, Figure 4 is an attempt to establish how ubiquitous this re-ignition behaviour might be. The diagram shows a series of time-lagged composites of v' cross sections, at the time when a trough axis passed the 270 °E meridian at 70 kPa. This level was chosen to eliminate any complications associated with the boundary layer. The composites were based on six winter seasons of data, from the 1984–1985 winter to the 1989–1990 winter. Figure 4(b) shows the composite for zero time lag. A pattern of disturbances up and downstream of 270 °E has decreasing amplitude as distance from 270 °E increases. The phase tilt with height is stronger downstream of 270 °E, in the main storm track region, than upstream. Figure 4(a) is a composite with a 2 day lag, while (4c) has a 2-day lead. The generally eastward movement of the troughs across the 270 °E meridian, their intensification and their increasing low-level phase tilt as they move eastwards, are all clearly seen.

5. Conclusions

This study clarifies the relationship between the storm tracks defined in terms of seasonal mean Eulerian statistics, and the individual weather systems, which contribute to those statistics. The lifecycle model of storm tracks, which interprets the Eulerian statistics in terms of baroclinically unstable, growing disturbances
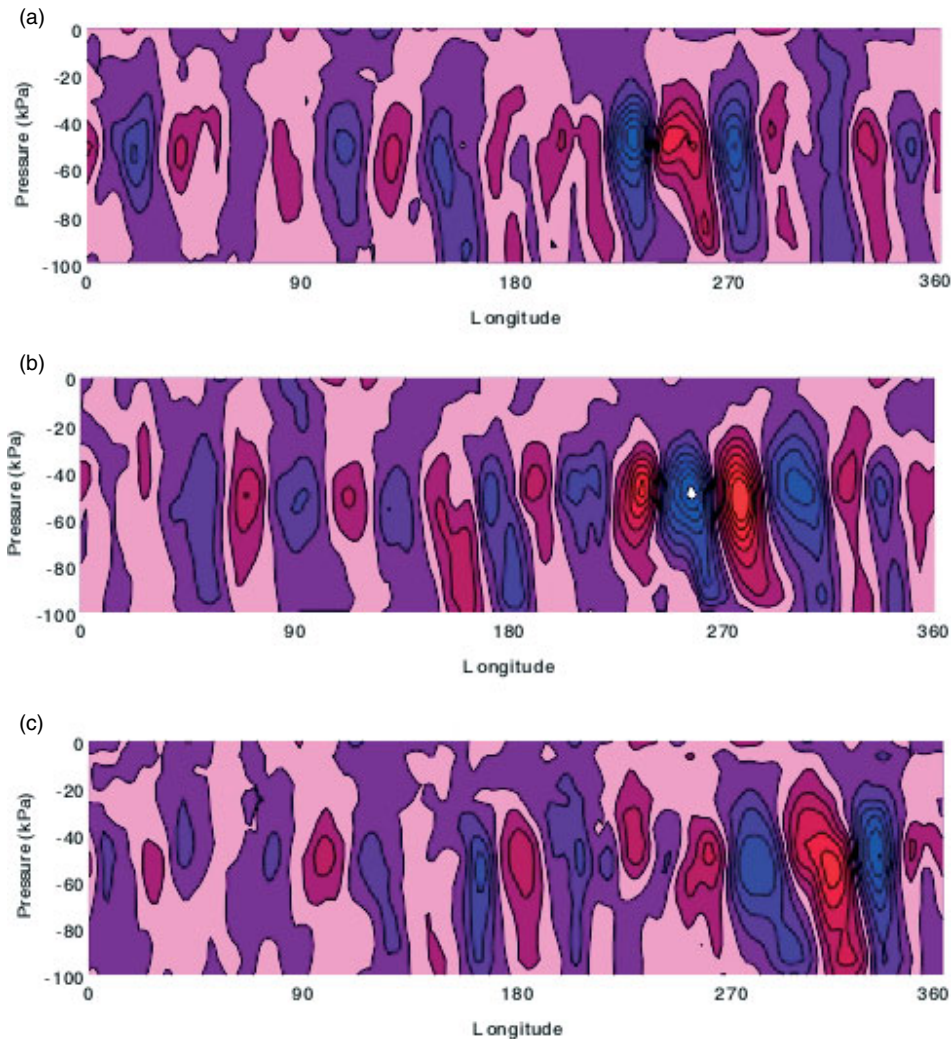
Figure 4. Composites from six winters from 1984 to 1985 to 1989–1990 of troughs crossing longitude 270 °E. (a) Lag 2 day composite. (b) Zero lag composite (c) Lead 2 day composite

at the western end of the storm track, and decaying disturbances at the eastern end of the storm track, is seen to be an oversimplification. While there may be a preponderance of growing systems to the west of the maximum of eddy kinetic energy, and a preponderance of decaying systems to its east, it is clear that very few disturbances grow or decay *in situ*. Rather, precursor systems enter the western end of the storm track and amplify somewhat as they pass through the storm track region. A significant remnant can be traced leaving the eastern end of the storm track. In many cases, these remnants enter the next downstream storm track, where they are 're-ignited', amplifying and then decaying once more. In this limited study of a single season, there is no example of a disturbance that grew from a very small amplitude within the storm track. Many other authors (see, e.g. Zhang and Held 1999, and references therein) have remarked on the importance of precursor disturbances entering the upstream end of the storm track region.

One implication of these results is that the North Atlantic and North Pacific storm tracks cannot really be regarded as separate, independent systems. At the tropopause level, there is hardly any break between the two storm tracks. Individual trough-ridge systems frequently pass from the Pacific into the Atlantic storm track, and there are significant numbers of convincing cases where systems can be followed from the Atlantic, right across Eurasia, to re-ignite in the Pacific storm track. A similar result has been shown by earlier authors: for example, Figure 2(a) of Chang (1993) shows comparable patterns to those in Figure 2 of this article.

Finally, we note that three-dimensional plots of the Eady baroclinic growth rate, not shown here, show two deep maxima, more or less coincident with the large temperature fluxes shown in Figure 1. Thus, local instability of the time-mean flow is indeed implicated in the formation of storm tracks. But the other crucial ingredient is the propagation of substantial upper level transient disturbances into the unstable region, as fuel for the re-ignition process. For example, we note that the winter reduction in activity in the Pacific storm track coincides with a reduction of the eddy activity

over central Eurasia. We suggest that the seasonal cycle of the Pacific storm track is related to the supply of precursor transients, not to local changes in the instability.

Acknowledgements

References

Blackmon ML. 1976. A climatological spectral study of the 500 mb geopotential height of the Northern Hemisphere. *Journal of the Atmospheric Sciences* **33**: 1607–1623.

Chang EKM. 1993. Downstream development of baroclinic waves as inferred from regression analysis. *Journal of the Atmospheric Sciences* **50**: 2038–2053.

Chang EKM, Lee S, Swanson KL. 2002. Storm track dynamics. *Journal of Climate* **15**: 2163–2183.

Hoskins BJ, James IN, White GH. 1983. The shape, propagation and mean-flow interaction of large scale weather systems. *Journal of the Atmospheric Sciences* **40**: 1595–1612.

Hoskins BJ, Valdes PJ. 1990. On the existence of storm tracks. *Journal of the Atmospheric Sciences* **47**: 1854–1864.

Hoskins BJ, Hodges KI. 2002. New perspectives on the northern hemisphere winter storm tracks. *Journal of the Atmospheric Sciences* **59**: 1041–1061.

James IN. 1995. *Introduction to Circulating Atmospheres*. Cambridge University Press: Cambridge, UK; 422.

James IN, Anderson DLT. 1984. The seasonal mean flow and distribution of weather systems in the southern hemisphere: the effect of moisture transports. *The Quarterly Journal of the Royal Meteorological Society* **110**: 943–966.

Nakamura H. 1992. Midwinter suppression of baroclinic wave activity in the Pacific. *Journal of the Atmospheric Sciences* **49**: 1629–1642.

Simmons AJ, Hoskins BJ. 1978. The lifecycles of some nonlinear baroclinic waves. *Journal of the Atmospheric Sciences* **35**: 414–432.

Simmons AJ, Hoskins BJ. 1980. Barotropic influences on the growth and decay of nonlinear baroclinic waves. *Journal of the Atmospheric Sciences* **37**: 1679–1684.

Trenberth KE. 1991. Storm tracks in the Southern Hemisphere. *Journal of the Atmospheric Sciences* **48**: 2157–2178.

Uppala SM, Kallberg PW, Simmons AJ, Andrae U, da Costa Bechtold V, Fiorino M, Gibson JK, Haseler J, Hernandez A, Kelly GA, Li X, Onogi K, Saarinen S, Sokka N, Allan RP, Andersson E, Arpe K, Balmaseda MA, Beljaars ACM, van de Berg L, Bidlot J, Bormann N, Caires S, Chevallier F, Dethof A, Dragosavac M, Fisher M, Fuentes M, Hagemann S, Holm E, Hoskins BJ, Isaksen L, Janssen PAEM, Jenne R, McNally AP, Mahfouf J-F, Morcrette J-J, Rayner NA, Saunders RW, Simon P, Sterl A, Trenberth KE, Untch A, Vasiljevic D, Viterbo P, Woollen J. 2005. The ERA-40 re-analysis. *The Quarterly Journal of the Royal Meteorological Society* **131**: 2961–3012.

Wallace JM, Lim G-H, Blackmon ML. 1988. Relationship between cyclone tracks, anticyclone tracks and baroclinic wave guides. *Journal of the Atmospheric Sciences* **45**: 439–462.

Zhang Y, Held IM. 1999. A linear stochastic model of a GCM's midlatitude storm tracks. *Journal of the Atmospheric Sciences* **56**: 3416–3435.